

# Pre-equilibrium $\gamma$ ray emission in different reaction mechanisms at $8\text{MeV/nucleon}$

M. Papa<sup>1</sup>, F. Amorini<sup>2,3</sup>, M. Cabibbo<sup>2,3</sup>, G. Cardella<sup>1</sup>, A. Di Pietro<sup>2,4</sup>, P. Figuera<sup>2</sup>, A. Musumarra<sup>2,5</sup>, G. Pappalardo<sup>2,3</sup>, F. Rizzo<sup>2,3</sup>, S. Tudisco<sup>2,3</sup>

<sup>1</sup> Istituto Nazionale di Fisica Nucleare – Sezione di Catania (Italy)

<sup>2</sup> Istituto Nazionale di Fisica Nucleare – Laboratorio Nazionale del Sud Catania (Italy)

<sup>3</sup> Dipartimento di Fisica Università di Catania (Italy)

<sup>4</sup> Department of Physics and Astronomy, University of Edinburgh JCMB, King's Building, Scotland

<sup>5</sup> CEA/DSM/DAPNIA/SPhN, Saclay, France

Received: 15 April 1998 / Revised version: 8 June 1998

Communicated by V. Metag

**Abstract.** Recent experimental results on particles- $\gamma$  coincidence measurements on the systems  $^{12}\text{C} + ^{64}\text{Ni}$  and  $^{35}\text{Cl} + ^{64}\text{Ni}$  at about  $8\text{MeV/nucleon}$  are interpreted as due to the effect of a Dipole pre-equilibrium emission produced during the damping of the proton-neutron relative collective motion in very deformed intermediate systems formed in the first instants of the collision. The pre-equilibrium effects are evaluated through semiclassical kinetic theories and through modified statistical approach to include non-stationary effects in Fusion processes, Massive Transfer reactions (in the  $^{12}\text{C} + ^{64}\text{Ni}$  system) and in Binary Dissipative reactions (in the  $^{35}\text{Cl} + ^{64}\text{Ni}$  system). In particular the study performed on the dipole molecular component allows to establish a link between the above phenomenon and the charge and mass transfer process in quasi-peripheral reactions.

**PACS.** 24.30.Cz Giant resonances – 25.70.-z Low and intermediate energy heavy-ion reactions

## 1 Introduction

In the last few years various experiments have been performed in which  $\gamma$ -rays have been detected in coincidence with charged particles produced in heavy ions reactions at  $E_{lab}/nucleon = 7 - 8\text{MeV}$  [1-6]. In some of these experiments [3-5] a production of  $\gamma$ -rays is evidenced over the GDR statistical contributions. The main characteristics of this extra yield are the relative low energy of the associated peak (around  $10\text{MeV}$ ) and the narrow width of a few  $\text{MeV}$ .

The aim of this paper is to discuss, in a first comprehensive study, the mechanism responsible for this emission giving also an estimation of the relative  $\gamma$ -ray emission probability. Through the comparison with statistical calculations, the important role played by the reaction mechanism on the visibility of this phenomenon is evidenced.

In particular we will focus our attention on the high energy  $\gamma$ -ray production observed in the  $^{35}\text{Cl} + ^{64}\text{Ni}$  [5] and  $^{12}\text{C} + ^{64}\text{Ni}$  [3,4] collisions. These experimental results will be briefly presented in Sect. 2.

In Sect. 3 the dynamical origin of the pre-equilibrium emission, as the result of the equilibration process for the proton vs. neutron collective motion is discussed.

In Sect. 4 a possible framework in which the pre-equilibrium and the statistical mechanism of emission can be included is presented. A way to estimate the corresponding emission probability is also indicated.

In Sect. 5 an estimation of the yield produced by a statistical emission is done for the two studied systems  $^{35}\text{Cl} + ^{64}\text{Ni}$  and  $^{12}\text{C} + ^{64}\text{Ni}$ . In these calculations the effect of the slow changing in time of the shape degree of freedom is also included.

In Sect. 6 the approach used in the study of the dynamical evolution of the process by means of the semiclassical kinetic theories, is briefly sketched. In the same part the results obtained for the studied systems in central and quasi-peripheral collisions are discussed and a comparison with the statistical calculations and with the experimental results is done.

In particular in order to describe the  $\gamma$ -ray spectrum measured in coincidence with the high energy  $\alpha$  particles produced in the  $^{12}\text{C} + ^{64}\text{Ni}$  collision, the role played by the cluster structure of the first excited states in the  $^{12}\text{C}$  nucleus is emphasized through Boltzman Noretheim Vlasov (BNV) calculations in which the projectile has been initialized as a  $3 - \alpha$  nucleus.

Sect. 7. contains the conclusive remarks.

## 2 Experimental results

In Fig. 1a we report one of the first claimed evidences [5] for non-statistical GDR  $\gamma$ -ray emission. In this figure the  $\gamma$ -ray spectrum measured in coincidence with the projectile-like produced in the deep inelastic reactions induced on the  $^{35}\text{Cl} + ^{64}\text{Ni}$  collision at  $7.74\text{MeV}/\text{nucleon}$  is shown.

The experimental results (points) are compared with the calculated statistical decay spectra of the fragments. In Fig. 1b the ratio between the experimental spectrum and the calculations are reported (points) together with a Lorentzian curve which best fits the points. From the figures is clearly seen an over strength centered at  $10\text{MeV}$  having a width of about  $3\text{MeV}$ .

More recently, by using the TRASMA detection system of the Laboratorio Nazionale del Sud (Catania) [7], we have studied the collision  $^{12}\text{C} + ^{64}\text{Ni}$  at  $7.9\text{MeV}/\text{nucleon}$ . A full description of the experimental results are given in [3,4]. Here we report, in Fig. 2a, the  $\gamma$ -ray spectrum collected in coincidence with fast  $\alpha$  particles (with energy greater than  $24\text{MeV}$ ) detected in the  $3^\circ \leq \theta_{lab} \leq 6^\circ$  angular range. The continuous line represents the calculated statistical contribution produced by the residual  $^{72}\text{Ge}$  nu-

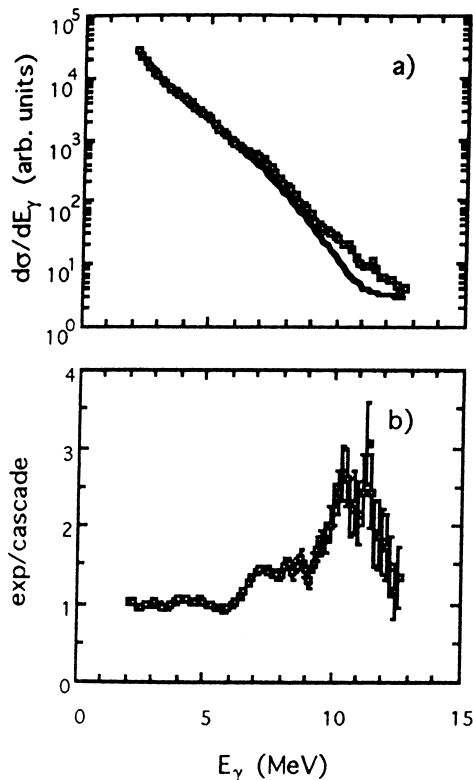


**Fig. 1.** **a** Experimental  $\gamma$ -ray spectrum (points) measured in the  $^{35}\text{Cl} + ^{64}\text{Ni}$  collision at  $7.7\text{ MeV}/\text{nucleon}$  in coincidence with binary dissipative events [5]. The solid line represents the result of CASCADE calculations (folded with the experimental set-up response function) applied to all possible primary fragmentation leading to the final detected fragments, **b** Ratio between the experimental data and the theoretical statistical calculations

cleus that we have supposed produced through a binary massive transfer process at the excitation energies which can be estimated through the two-body kinematic applied to the outgoing channel. The average value of both the excitation energy and of the total transferred angular momentum are about  $59\text{MeV}$  and  $\langle J \rangle = 24\hbar$  respectively [3].

In Fig. 2b we show the ratio between the statistical calculation and the experimental data. Also in this case it is clearly seen an over production of  $\gamma$ -rays at an energy of about  $10\text{MeV}$  with a F.W.H.M of about  $2\text{MeV}$ .

Finally in Fig. 3 we show, for the same reaction, the  $\gamma$ -ray spectrum collected in coincidence with the evaporation residues [3]. The solid and dashed lines represent, as above, statistical calculation performed by using the code CASCADE. In Table I the parameter values obtained from the fit procedure are also reported. In this case the agreement between the statistical calculation and the experimental data seems good enough and no clear effect of a pre-equilibrium emission is evidenced. On the contrary this kind of analysis evidences some degree of uncertainty in the selection of the starting guess for the fit procedure (for example one or two Lorentzian strength distributions to describe the decay of the GDR).

From the previous comparisons some new and interesting aspects about the high energy  $\gamma$  emission can be evidenced.

The first aspect is the “anomalous” high energy  $\gamma$ -ray production as shown in Figs. 1 and 2. This process can be connected to a pre-equilibrium emission as we will discuss in the following.

The second one concerns the link between this phenomenon and the reaction mechanisms. In the data here presented in fact this “anomalous” emission is clearly evidenced in peripheral or quasi-peripheral reactions whereas this does not happen for the studied  $^{12}\text{C} + ^{64}\text{Ni}$  system in more central collisions leading to fusion, as evidenced from the inspection of Fig. 3.

Before to conclude this section we have to quote also the experimental results presented in [8]. In that work evidences of a pre-equilibrium emission have been obtained at lower incident energy ( $E_{lab}/\text{nucleon} = 4.25 - 4.5\text{MeV}$ ) and in central collisions selected by  $\gamma$ -ray multiplicity and spectroscopy measurements.

We begin the study of this phenomenon briefly discussing, in the next section, the possible source of pre-equilibrium emission.

## 3 Dynamical origin of the Pre-equilibrium emission

In several papers published in these last years [9-11] a source of pre-equilibrium  $\gamma$  emission in heavy ions collisions has been associated to the charge over mass asymmetry in the entrance channel. In the following we discuss briefly this aspect having in mind the study of the pre-equilibrium emission in quasi-peripheral collisions in which highly deformed systems can be produced.

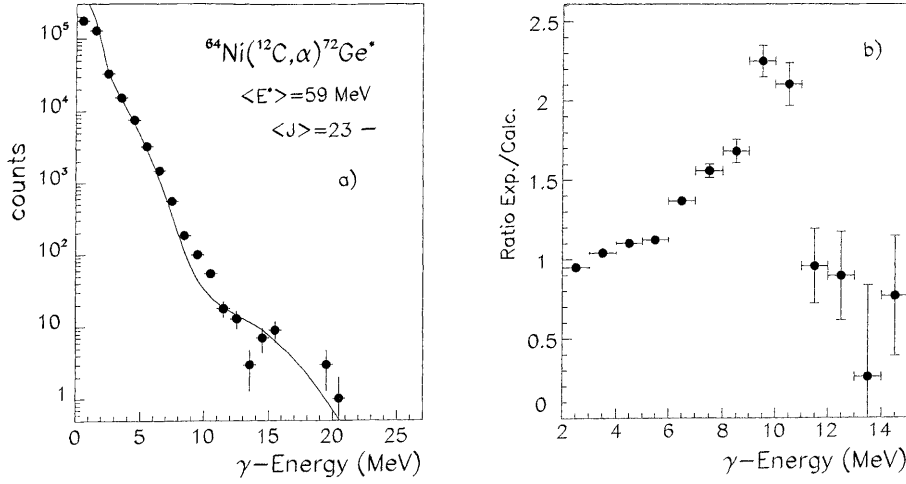


**Fig. 2.** **a** Experimental  $\gamma$ -ray spectrum (points) measured in the collision  $^{12}\text{C} + ^{64}\text{Ni}$  at 7.9 MeV/nucleon in coincidence with fast  $\alpha$  particles ( $E_\alpha \geq 24\text{MeV}$ ) detected in the angular range  $3^\circ \leq \theta_{lab} \leq 6^\circ$  [3,4]. The solid line represents the result of CASCADE calculations (folded with the experimental set-up response function) applied to the residual nucleus  $^{72}\text{Ge}$ . The average values of the excitation energy  $\langle E^* \rangle$  and total spin  $\langle J \rangle$  as estimated through the two body kinematics are also reported, **b** Ratio between the experimental data and the theoretical statistical calculations

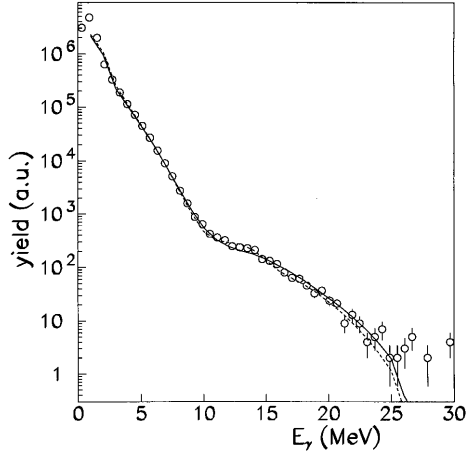


**Fig. 3.** Experimental  $\gamma$ -ray spectrum (points) measured in the  $^{12}\text{C} + ^{64}\text{Ni}$  collision at 7.9 MeV/nucleon in coincidence with evaporation residues [3,4]. The lines represent a result of CASCADE calculations, folded with the experimental set-up response function, applied to the Compound Nucleus. The solid and dashed lines refer to calculations in which the GDR strength is described through one Lorentzian and two Lorentzian distributions respectively. The set of parameters obtained by the fit procedure are reported in Tab. 1

To this aim we explicit the expression of the total electrical dipole (per unit of elementary charge) for a system which is divided into two subsystems having mass and charge  $A_p, Z_p$  and  $A_t, Z_t$  respectively (the reference is the center of mass of the total system):

$$\mathbf{D} = \sum_{Z_p+Z_t} \mathbf{r}_i = \mathbf{D}_p + \mathbf{D}_t + \mathbf{D}_m \quad (3.1)$$

$$\mathbf{D}_p = \frac{N_p}{A_p} \sum_{Z_p} \mathbf{r}_i - \frac{Z_p}{A_p} \sum_{N_p} \mathbf{r}_i$$

$$\mathbf{D}_t = \frac{N_t}{A_t} \sum_{Z_t} \mathbf{r}_i - \frac{Z_t}{A_t} \sum_{N_t} \mathbf{r}_i \quad (3.2)$$

$$\mathbf{D}_m = Z_p \mathbf{R}_p + Z_t \mathbf{R}_t \quad (3.3)$$

The terms  $\mathbf{D}_p$  and  $\mathbf{D}_t$  are the intrinsic dipole's of the subsystems.

The third term in (3.1) represents the so called molecular dipole,  $\mathbf{R}_p, \mathbf{r}_{cm}$  are the center of mass vectors (C.M.) of the two subsystems. This term, by definition, is always oriented along the direction defined by the centers of mass of the two subsystems.

Since the position of the C.M. of the total system is located at the origin of the coordinate system, we can also write:

$$\mathbf{D}_m = \frac{A_p A_t}{2(A_p + A_t)} \left( \frac{(Z_p - N_p)}{A_p} - \frac{(Z_t - N_t)}{A_t} \right) \times (\mathbf{R}_p - \mathbf{R}_t) \quad (3.4)$$

The illustrated decomposition is well suitable to represent the situation of two interacting nuclei. In particular at  $t=0$ , when they start to strongly interact, the only term that can be different from zero, apart from polarization effects, is just the molecular contribution and this happens only if the interacting particles have different charge to mass asymmetry.

The definition (3.4) shows how  $\mathbf{D}_m$  can be expressed through collective quantities connected to the relative motion of the two partners.

Fast changes in time of this quantity are expected during the interaction and they are due only to the charge to mass asymmetry variation between the two partners.

At this point we want to precise that, even if the above decomposition is possible at each time (to obtain it in fact we have applied simple algebra), it is not possible, in general, to obtain a distinct time behaviour of the three terms because the dynamical evolution strongly couples all the degrees of freedom of the system. In spite of that, in particular conditions like peripheral or quasi-peripheral collisions (i.e. collisions in which the two partners don't lose completely their identity), the coupling can be less effective due to the centrifugal and Coulomb forces and the  $\mathbf{D}_m$  can become prominent showing clearly the proper evolution.

Finally we observe that by accelerating ions with different charge to mass asymmetry we displace neutron and

proton spheres also in the momentum space. This displacement corresponds to a C.M. relative momentum:

$$\Delta P_{Z,N} = P_L \left( \frac{(Zp - Np)}{Ap} - \frac{(Zt - Nt)}{At} \right) \quad (3.5)$$

Where  $P_L$  is the projectile linear momentum in the laboratory system. At  $7 - 8\text{MeV}/\text{nucleon}$  the kinetic energy of the proton vs. neutron relative motion is only about  $2\text{MeV}$  for the studied systems and instead of therefor it is not enough large to excite the corresponding mode. Therefore, in this case, the main mode to dynamically excite the GDR is trough the displacement in the configuration space which corresponds the so called molecular dipole.

## 4 General-framework

To make a comparison between a statistical decay mechanism and a pre-equilibrium one it is necessary to work in a general framework in which these two mechanisms can be included. Such a framework can be taken from the multistep reaction theories [12] which have been developed and successfully applied to the description of light particles-heavy ions collisions. This framework has been applied in [10,13,14] to the gamma decay by using the phonon concept.

On the other hand in the present paper we will use semiclassical calculations based on mean field kinetic theories, so we feel the necessity, from a formal point of view, to describe the pre-equilibrium process and the compound system decay in the typical framework of a multistep process in which the complexity of the phase space is ordered according to the average collective energy associated to the proton-neutron motion.

As shown in Appendix A in this case it is possible to express the total probability of  $\gamma$  emission as

$$\frac{dP^\gamma}{dE_\gamma} = \frac{W_S^\gamma}{T_S} \left( \frac{\Gamma_D^\downarrow}{\Gamma_D} \right) + \frac{W_D^\gamma}{\Gamma_D} = S_s(E_\gamma) + S_d(E_\gamma) \quad (4.1)$$

In the above expression the first term represents the statistical contribution coming from the last stage of the process. The factor  $\frac{W_S^\gamma}{T_S}$  gives the  $\gamma$  emission probability from a C.N. in the GDR region. It is evaluated by using the principle of the detailed balance which can be applied because of the statistical equilibrium hypothesis on the proton vs. neutron motion; it is the ‘‘heart’’ of statistical CASCADE calculations [15].

The consequences of this principle are that  $W_S^\gamma$  explicitly contains the level density factor and that it is computed trough the cross section  $\sigma_{abs}(E_\gamma)$  for  $\gamma$  absorption which satisfies the well known sum rule:

$$W_S^\gamma = \frac{\rho(E_i, J_i, \pi_i)}{\rho(E_f, J_f, \pi_f)} \frac{\sigma_{abs}(E_\gamma) E_\gamma^2}{3(\pi \hbar c)^2} \quad (4.2)$$

The factor in the brackets of (4.1) represents the loss of flux due to the pre-equilibrium stage: it is defined trough

$\Gamma_D$  and  $\Gamma_D^\downarrow$  which represent the total and the damping decay constants of the pre-equilibrium process respectively ( $\Gamma_D = \Gamma_D^\downarrow + \Gamma_D^\uparrow$ ). As shown in Appendix A, in a simple 3 stage process, they are (apart from the coupling to the continuum  $\Gamma_2^\uparrow$ , see Appendix.A) the reduced values of the parameters characterizing the decay of the two classes belonging to the pre-equilibrium process (see (A.11) and (A.12)). Then already at this level we can expect, in the classical-quantum analogy, a reduction of the width connected to the  $\gamma$ -ray emission as due to time evolution of the process i.e to the finite time for Compound Nucleus (C.N.) formation.

We could compare this effect to the motional narrowing [16] occurring in resonant processes undergoing time dependent perturbations.

From an experimental point of view the statistical contribution can be reduced by selecting reaction mechanisms in which the equilibrium stage is strongly suppressed by a small value of  $\Gamma_D^\downarrow$  or/and low effective temperature like in the Deep Inelastic Collisions (D.I.C.). This allows to put clearly in evidence the  $\gamma$ -ray emission coming from the pre-equilibrium stage as we will show in the following.

The second term of (4.1) represents the dynamical pre-equilibrium contribution. We will estimate the associated  $\gamma$ -ray emission by evaluating the power emitted from the total dipole during the equilibration process by means of the semiclassical kinetic theory. This will be done by solving the BNV equation. In particular from the time dependence of the  $i$  total dipole component  $D_i(t)$ , the corresponding probability to emit a  $\gamma$ -ray in the energy interval  $E_\gamma, E_\gamma + dE_\gamma$  can be expressed using the electrodynamics laws, as:

$$\begin{aligned} S_d(E_\gamma) dE_\gamma &= \frac{W_{D,i}^\gamma(E_\gamma)}{\Gamma_D} dE_\gamma \\ &= \frac{4}{3} \left( \frac{e^2}{\hbar c} \right) \left( \frac{E_\gamma}{\hbar c} \right)^3 |D_i(E_\gamma)|^2 dE_\gamma \end{aligned} \quad (4.3)$$

where

$$D_i(E_\gamma) = \frac{1}{c} \int_{0,\infty} D_i(\tau) e^{-i \frac{E_\gamma}{\hbar c} \tau} d\tau \quad (4.4)$$

is the Fourier transform of  $D_i(t)$

Therefore we will not apply the reciprocity principle because in the above defined pre-equilibrium stage the collective proton-neutron motion is not equilibrated.

## 5 Statistical decay

Before showing the results of the semiclassical calculations we present in Fig. 4 and 5 the prediction of the statistical model.

In Fig. 4 we show the GDR  $\gamma$  emission probability for the compound system  $^{12}\text{C} + ^{64}\text{Ni}$  at  $7.9\text{MeV}/\text{nucleon}$  which corresponds to a temperature of about  $3\text{MeV}$ . The displayed results have been obtained performing a weighted sum over all the partial waves contributing to fusion. The different curves are referred to calculations in

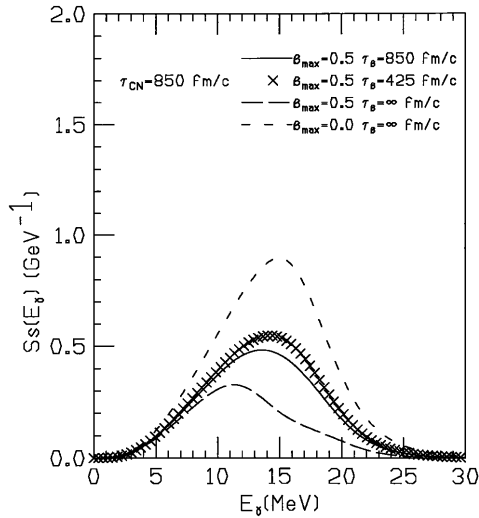


**Fig. 4.** One-step statistical model yields evaluated by means of the equations B.2 and B.3 for the  $^{12}\text{C} + ^{64}\text{Ni}$  intermediate system. In the figure the parameters associated to the different curves are also reported. The interval of total angular momenta considered is  $J = 0 - 75$  ( $\hbar$  unit)

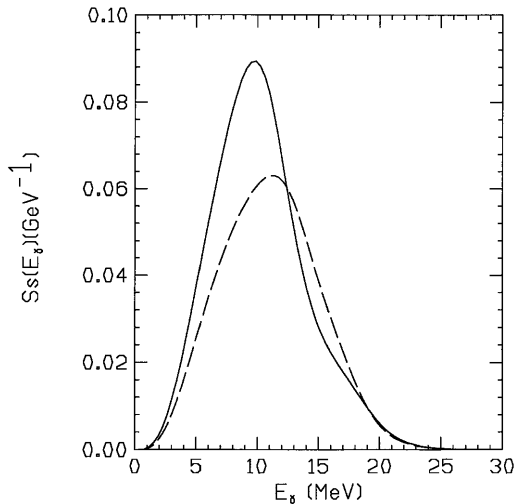


**Fig. 5.** One-step statistical model yields evaluated by means of the equations B.2 and B.3 for the  $^{35}\text{Cl} + ^{64}\text{Ni}$  system. The figure is referred to a dinuclear system in a “sticking” configuration. The different lines are relative to different value of the low energy resonance  $E_{GDR}$ . The total angular momentum is fixed to  $J = 76$  ( $\hbar$  unit). As in the calculations shown in Fig. 4, the value of the high energy resonance has been evaluated from  $E_{GDR}$  by supposing the weighted between the low and the high energy modes (1/3 low energy, 2/3 high energy) equal to the resonance energy of the spherical system

which we have included, in the local equilibrium hypothesis, non-stationary effect as due to the slow change in time of the deformation parameters. The maximum value of the quadrupolar degree of freedom the associated relaxation time  $\tau_\beta$  and the C.N. average life time  $\tau_{CN}$  are shown in the same figure. Apart from these effects, which give rise to a kind of “Pre-equilibrium-Statistical emis-

sion” and that are fully discussed in Appendix B, we note that the intensity at the maximum of the yield distribution is of the order of  $5 - 7 \times 10^{-4} \text{MeV}^{-1}$ .

We furthermore note that the widths of the distributions are in each case well above  $5\text{MeV}$  (see Appendix B).

In Fig. 5, as an example, we show similar calculations for the  $^{35}\text{Cl} + ^{64}\text{Ni}$  system at  $7.7\text{MeV}/\text{nucleon}$ , formed in a sticking configuration with fixed total angular momentum  $J=76\hbar$  greater than the critical one. This configuration can represent a dinuclear system formed in a D.I.C. process at an impact parameter equal to 5.5 fm as suggested by dynamical calculations (see Sect. 6). In this case the emission probability is of the order of  $10^{-5} \text{MeV}^{-1}$  because of the Coulomb and deformation effects, which are able to lower the effective temperature. The widths are about  $10\text{MeV}$ .

Therefore due to the relatively large value of the width produced by the statistical emission as compared with the experimental result, we can already conclude that this kind of emission can not be the source of the over production we are discussing.

## 6 Dynamics of the process

To study the dynamical evolution of the process by using a microscopic approach it is possible to use, as well known, only approximated methods to the solution of the quantum-mechanical many-body problem. Several schemes of approximations have been applied to the heavy ion collisions depending on the energy of the impinging nuclei. At the lower energies TDHF theory has been applied to the heavy ion collisions and theoretical investigation have shown [17] that such a quantal mean field theory is able to describe the very initial phase of the reaction up to about  $20\text{MeV}/\text{nucleon}$ .

The effect of the residual interaction which develops on a successive stage and which is one of the mechanisms responsible of the dissipation effects in the collective dynamics has been treated in a variety of methods because of the numerical difficulties connected to the calculation based on a generalized or extended TDHF theory.

A part from the non-equilibrium statistical transport theories the Dissipative Diabatic Dynamics (DDD)[18] both in the semiclassical and quantum-mechanical version (see for example [19,20]) solves the evolution of the slow collective nuclear motion by introducing explicitly the collective degree of freedoms and by defining diabatic single particles basis and the associated Hamiltonian.

On the other hand fully microscopic approaches based on semiclassical kinetic theories like BUU, VUU, and BNV[21] have been successful applied [21-26] in the same energy domain ( $10-20\text{MeV}/\text{nucleon}$ ) to take into account the effects on the average dynamics.

Even if the more sophisticated DDD approach, depending on a number of ansatzes, describes memory effects, quantal and classical fluctuations, we will use in the following a microscopic semiclassical description based on

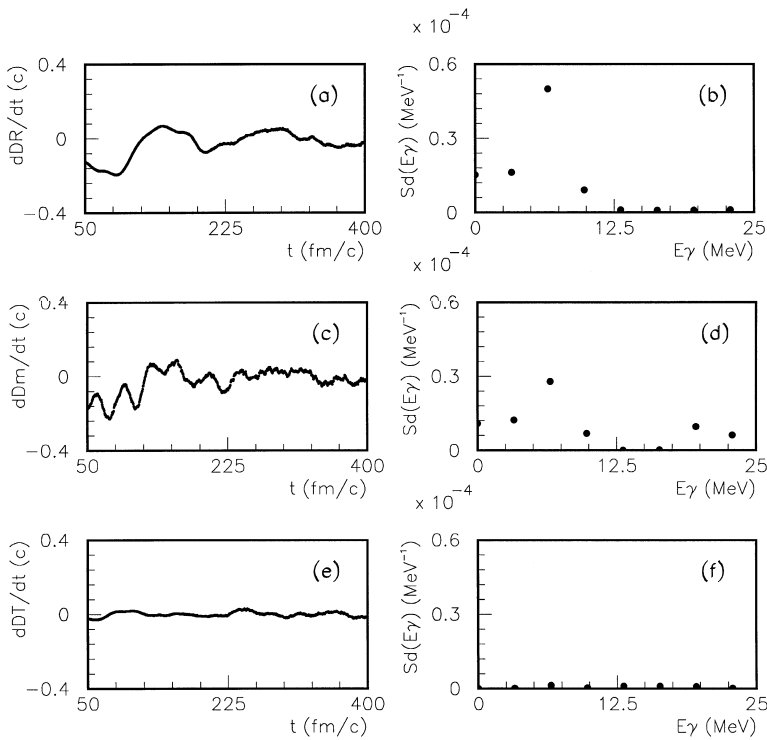


**Fig. 6.** a–f. Results of B.N.V. calculations for the  $^{35}\text{Cl} + ^{64}\text{Ni}$  system at 7.7 MeV/nucleon and at an impact parameter  $b=5.5\text{fm}$ , **a** first time derivative of the total radial dipole as function of time, **b** associated emission probability distribution as function of the  $\gamma$ -ray energy. It has been computed through the equations 4.3 and 4.4, **c**, **d** the same quantities are plotted for the molecular component respectively, **e**, **f** the same quantities are plotted for the transversal component respectively

the BNV equation, in the full spirit of the semiclassical approximation.

### 6.1 Semiclassical calculations

In order to follow the time evolution of the system we have performed semiclassical calculations based on the BNV equation.

The nuclear mean field has been described through a density functional of the Skyrme type corresponding to a soft EOS:

$$U(\rho) = -\frac{356}{\hbar c} \frac{\rho}{\rho_0} + \frac{303}{\hbar c} \left(\frac{\rho}{\rho_0}\right)^{4/3} + \frac{38}{\hbar c} \left(\frac{\rho_p - \rho_n}{\rho_0}\right) \quad (6.1)$$

Coulomb interaction has been also taken into account.

The BNV equation has been solved by using the test-particles method [21]. We have used 1000 test particles per nucleon. Such a large number makes the spurious oscillations in the dipolar components, as due to the numerical noise, negligible in the first 500 fm/c.

The nucleon-nucleon cross section has been described according to [21]. Due to the simple parameterization of the mean field and nucleon-nucleon cross section (we neglect the momentum dependent effects) this assumption can be regarded as a first step of approximation. Nevertheless this kind of mean field and nucleon-nucleon cross section have been frequently used in the literature to study the dynamics of heavy ions collision also at low energy  $E_{lab}/A \leq 10\text{MeV}$  (see for example [9,24-26]). In particular, as shown in (6.1), we have considered the most important mean field term for the proton vs. neutron collective motion through the charge to mass asymmetry term.

In order to obtain the time evolution of the dipole operator in all its components, we have divided at each time step the total system into two subsystems. At  $t = 0$  these subsystems are the projectile and the target while for the following time steps they change according to the following criterion: a test particle belongs to subsystem 1 if its distance from the C.M. of cluster 1 is smaller than the distance from the C.M. of the cluster 2. Otherwise it belongs to the cluster 2. This procedure will be useful to describe peripheral and quasi-peripheral collisions and it will produce the collective new variables  $Z_{1,2}(t)$ ,  $N_{1,2}(t)$ ,  $\mathbf{R}_{cm,1,2}(t)$  corresponding to the number of neutrons and protons belonging to the projectile-like, target-like fragments and the relative center of mass coordinates.

Obviously in this way it is possible to define a radial direction along the C.M. of the two subsystems and a transversal one. This last one will be orthogonal to the radial direction and parallel to plane defined by the beam ( $\hat{z}$ ) and the impact parameter direction ( $\hat{x}$ ).

### 6.2 $^{35}\text{Cl} + ^{64}\text{Ni}$ $E_{lab}/nucleon = 7.7\text{MeV}$ – Deep inelastic collision

For this system we have already presented in Sect. 2 (see Fig. 1a and Fig. 1b) the energy spectrum of the  $\gamma$ -rays detected in coincidence with binary dissipative reaction and the comparison with the statistical calculations applied to all the possible primary fragmentations [5].

In Fig. 6 the results obtained for an impact parameter of 5.5 fm are shown. This run produces a dinuclear system which lives about 500 fm/c.

In Fig. 6a and Fig. 6c we display, the first time derivative for the total radial dipole  $DR$  and the molecular one as function of time.

The time scale offset of about 50 fm/c represents the time interval in which the two nuclei, starting from the initial configuration of the BNV simulation (relative distance  $D_{CM} = 13fm$ ), reach a relative distance  $D_{CM} = 1.1(R_p + R_t)$  ( $R_p, R_t$  projectile and target nuclear radii). Therefore in the following analysis we will not take into account the approach phase being interested to the resonant processes. Nevertheless we have verified that the approach stage will sensibly modify the  $\gamma$ -ray emission spectra (about 20% of the total resonant yield) only in the low energy region  $E_\gamma \leq 6MeV$  as result of the Bremsstrahlung effect.

In Fig. 6b and Fig. 6d we show the emission probability spectrum for the total radial dipole and the molecular component respectively, computed in the 50–400 fm/c time interval. A concentration of strength is visible around  $E_\gamma \simeq 8MeV$ . The ratio between the two contributions is about 50%. The low frequency value obviously reflects the fact that a highly deformed dinucleus is formed. From a reaction mechanism point of view, this means that a noticeable fraction of the low energy GDR is associated to the charge and mass transfer between the two partners (see (3.4)). The connection between the excitation of the molecular component and the transfer mechanism is also understandable through the fact that during the interaction time the distance  $D_{CM}$  between the two quasi nuclei does not show an oscillating behaviour as can be seen in Fig. 7a, in fact the quasi periodicity of the molecular terms can be attributed only to the changes in time of the charge to mass asymmetry  $y = \frac{Z_p(t)}{A_p(t)} - \frac{Z_t(t)}{A_t(t)}$  between the two partners as shown in Fig. 7b.

The transversal component  $DT$ , as displayed in Figs. 6e and 6f, is very weakly excited according to the observation done at the end of Sect. 3.

The widths of the emission probability distributions are about 3–4MeV. With regard to this from the BNV simulations it results that the rate of nucleon-nucleon collision reaches its maximum and stationary value after a time interval of about 120 fm/c. We have verified that this delay corresponds approximately to the time interval elapsed after each particles of the quasi-projectile has interacted with at the least one particles of the quasi-target. It is strongly affected by the Pauli-blocking, by the mean field and then also by the shape of the system in the pre-equilibrium stage. This time interval has also a finite value in central collision even if its value is smaller (about 70 fm/c as evaluated in the  $b=0$   $^{12}C + ^{64}Ni$  simulation) mainly because of the smaller centrifugal and Coulomb potentials. Obviously this time delay, together with the pronounced time dependence of the mean field, plays a crucial role in to weak the damping of the neutron-proton collective motion in the pre-equilibrium phase of the collision.

To conclude this subsection we make the comparison of the dynamical calculations with the statistical model and with the experimental results.

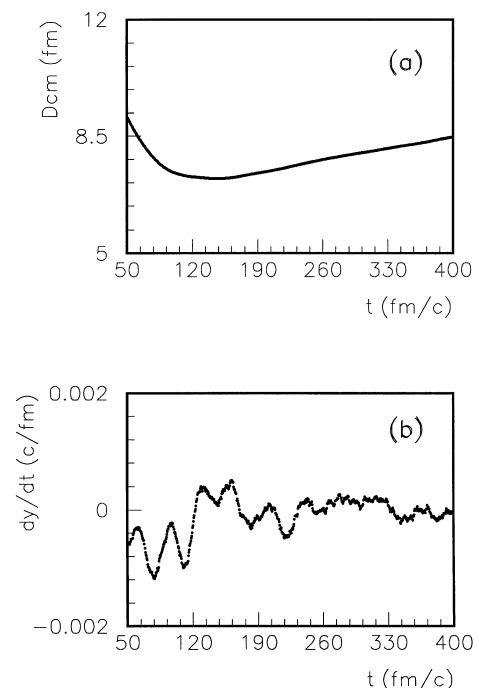


**Fig. 7. a, b.** Results of B.N.V. calculations for the  $^{35}Cl + ^{64}Ni$  system at 7.74 MeV/nucleon and at an impact parameter  $b=5.5$  fm, **a** Distance between the two quasi-fragments as function of time, **b** The first time derivative of the quantity  $y = \frac{Z_p(t)}{A_p(t)} - \frac{Z_t(t)}{A_t(t)}$  is plotted as function of time

The peak of the dynamical contribution gives a strength of about  $6 \times 10^{-5} MeV^{-1}$ . In Fig. 5, in which we have shown the statistical model predictions, the curves with solid and dashed lines represent contributions from an angular momentum value corresponding to the impact parameter used in the BNV simulation. We can see a width of about 10MeV and a strength at the peak position equal to  $9 \times 10^{-5} MeV^{-1}$  or  $6 \times 10^{-5} MeV^{-1}$  depending on the GDR energy which has been considered a free parameter set to reproduce the experimental peak position (about 10MeV).

For the sake of completeness in this comparison we have also to take into account the attenuation in the statistical emission rate due to the presence of the dynamical pre-equilibrium emission. To estimate the ratio  $\frac{\Gamma_D^\perp}{\Gamma_D}$  we have considered a  $\Gamma_D$  value of 2.5MeV (as suggested from the data; see Fig.1b)); considering a dinuclear system mean life time of about 500fm/c (as suggested by the dynamical calculation), the value of  $\Gamma_D^\perp$  is 0.8MeV. Therefore the resulting attenuation factor is about 0.7.

Then the ratio at the peaks positions between the dynamical contribution and the statistical one can reach now a value greater than 1.

Moreover the width of the dynamical contribution is about 4MeV, which is in reasonable agreement with the experimental value within the indetermination of the Fourier analysis.

Therefore the results presented in this section clearly indicate: i) deep inelastic reactions are a good tool to show up the pre-equilibrium dynamical emission; ii) the dynamical emission is strongly linked in this case with the charge and mass transfer mechanism.

### 6.3 $^{12}\text{C} + ^{64}\text{Ni}$ $E_{\text{lab}} = 7.9\text{MeV/nucleon}$ - Fusion process

In the present section we want to compare the experimental results obtained in the  $^{12}\text{C} + ^{64}\text{Ni}$  collision at  $7.9\text{MeV/nucleon}$  with the prediction of the already sketched approach. In Sect. 2 we have already presented the  $\gamma$ -rays energy spectrum produced in coincidence with evaporation residues detected in the forward direction (see Fig. 3) whose shape is in agreement with the C.N. statistical decay.

In Fig. 8 we present, as an example, the results of BNV calculations for a central collision. In Fig. 8a we report the first time derivative of the dipole component as function of time along the beam direction  $\hat{z}$ . In Fig. 8b we also show the corresponding probability of  $\gamma$  emission per unit energy.

The oscillations decay in about  $120\text{ fm/c}$  which corresponds to a width in the probability distribution of about  $3.5\text{MeV}$ , but the strength distribution is more large and the F.W.H.M is about  $6\text{MeV}$  because the system explores

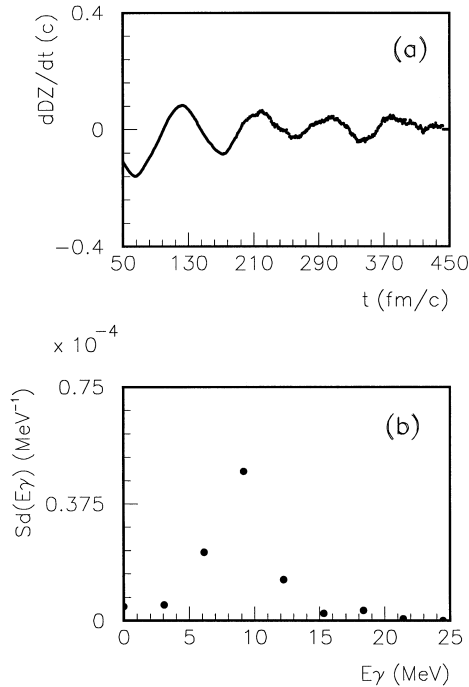


**Fig. 8. a, b.** Results of B.N.V. calculations for the  $^{12}\text{C} + ^{64}\text{Ni}$  system at  $7.9\text{ MeV/nucleon}$  and at an impact parameter  $b=0\text{ fm}$ , **a** first time derivative of the total dipole along the  $\hat{Z}$  direction as function of time, **b** associated emission probability distribution, as function of the  $\gamma$ -ray energy, is plotted. It has been evaluated through the relations 4.3 and 4.4

different deformation until the collective proton-neutron motion reaches the equilibrium.

In this case we have a probability at the peak energy of the order of  $4 \times 10^{-5}\text{MeV}^{-1}$ , which is about one order of magnitude lower than the statistical contribution (see Sect. 5) Also others calculations, performed at different impact parameters involved in the fusion process, give the same order of magnitude. For the studied system we can therefore understand why no over strength is clearly observed in the  $\gamma$ -ray energy spectrum in coincidence with a large class of evaporation residues and, more generally, how in fusion reactions at this energy the search of pre-equilibrium  $\gamma$  emission due to the equilibration of the proton v.s. neutron motion, could be masked by the large statistical contribution due to the compound nucleus formation.

### 6.4 $\alpha - \gamma$ coincidence measurements in the $^{12}\text{C} + ^{64}\text{Ni}$ collision at $E_{\text{lab}} = 7.9\text{MeV/nucleon}$ - Massive transfer reaction

In the  $^{12}\text{C} + ^{64}\text{Ni}$  collision we detected also  $\alpha$  particles with energy around the value corresponding to the beam velocity. Also  $^8\text{Be}$  particles are produced in the same angular range, they have been identified by looking at  $2\alpha - \gamma$  coincidence events [3].

A carefully analysis on the  $^8\text{Be}$  events has shown that their contribution to the  $\alpha - \gamma$ -ray coincidence energy spectrum shown in Fig. 2a is about 15%, moreover this fraction becomes negligible for the  $\gamma$ -ray yield around  $10\text{ MeV}$ . In this figure the solid line represents the result of calculations performed with the code CASCADE applied to the excited residual nucleus obtained through the transfer of  $^8\text{Be}$  (see Sect. 2)

As can be seen, statistical model applied to the outgoing channel underestimate the yield in the region around  $10\text{ MeV}$

From the data we can calculate, by subtracting the statistical contribution, an effective emission probability due to the pre-equilibrium stage equal to about  $2 \times 10^{-4}\text{MeV}^{-1}$  at the maximum of the distribution.

With this respect, all the possible checks have been performed to exclude the possibility that the  $\gamma$ -rays, at about  $10\text{MeV}$ , rise from  $^{12}\text{C}$  target contamination or from the decay of some particular level in the excited residual nucleus [3]. From this evidence we can conclude that the fast process we are faced in, which we can include in the wide class of transfer reactions, strongly selects the excitation of the dynamical mode under study.

Moreover it is reasonable, due to the  $\alpha$  and  $^8\text{Be}$  yields, that the cluster structure of the first excited states in the light  $^{12}\text{C}$  nucleus plays an important role in the transfer process. This interpretation is confirmed by other studies on the  $^{12}\text{C}$  induced reactions [27,28].

On the other hand normal BNV calculations, at this incident energy, are not able to reproduce  $\alpha$  particles in the outgoing channel. Up to an impact parameter of about  $5\text{ fm}$  the calculation predicts the fusion of the two incoming particles and at higher impact parameters quasi-elastic



reactions are obtained in which a quasi-projectile is produced.

With this regard we have to observe that recently Antisymmetrized Molecular Dynamics approach has been used to describe alpha clustering effects in  $^{12}\text{C}$  fragmentation processes induced through heavy ion collisions at  $E_{\text{lab}}/\text{nucleon} \geq 22\text{MeV}$  [28]. On the other hand we are interested mainly to the collective dipolar mode during the transfer stage for which a mean field approach is more fundamental.

Therefore in order to interpret the experimental data by the approach insofar used we have tried to describe with semiclassical calculations, based on BNV equation, a  $3 - \alpha$   $^{12}\text{C}$  projectile.

As it is well known the many-body correlations responsible for clustering in light nuclei are, by definition, absent in mean field theories. Then we can only introduce this correlation at  $t=0$  and find the right configurational parameter values to get a metastable state which survives so long to play an important role in the dynamical evolution of the process.

Therefore in this case we are assuming like a starting hypothesis the excitation of substructures in the  $^{12}\text{C}$  nucleus.

From spectroscopy and  $\alpha$  decay studies we know that some of the first excited states of the  $^{12}\text{C}$  (for example  $7.65\text{MeV}(2^+, 0^+)$ ,  $9.64\text{MeV}(3^-)$ ) have been described through a mixing of  $3 - \alpha$  clustered structures in which the equilateral triangular structure plays a dominant role [29-31].

Starting from these considerations we have prepared the initial state of the  $^{12}\text{C}$  in a BNV simulation by imposing restrictions on the nuclear density. We have distributed test particles around the vertexes of an equilateral triangle to build  $3 - \alpha$  particles with radius  $r_0 = 1.78\text{fm}$  and inside a Fermi sphere of  $k_f = 0.7\text{fm}^{-1}$ .

The distance between the vertex  $d_{cl}$  has been fixed by imposing a stable configuration up to  $100\text{fm}/c$ . This procedure gives  $d_{cl} \simeq 2.5r_0$ .

The evaluated excitation energy is about  $10\text{MeV}$ . After this we have chosen the orientation of the  $3 - \alpha$  triangle by minimizing the Coulomb interaction with the target. For a fixed distance between the C.M. of the two partners and for impact parameters less than  $5\text{fm}$ , the minimum has been found to correspond to a configuration in which the  $3 - \alpha$  particles stay on a plane orthogonal to the reaction plane with one vertex on the axes defined by the impact parameter direction.

In particular in our calculation we have verified that the  $\alpha$ -particles interact weakly through the tails of the nuclear matter density and through the Coulomb interaction but at the same time each of them is strongly bound through the mean-field and through the Pauli principle which at  $t=0$  prevents the action of the residual interaction.

In Fig. 9 we show a two-dimensional plot (in the reaction plane) of the nuclear density for the collision  $^{12}\text{C}^* + ^{64}\text{Ni}$  at  $b=4.7\text{fm}$  at different times as indicated in the pictures. At  $t=0$  it is possible to observe the rep-

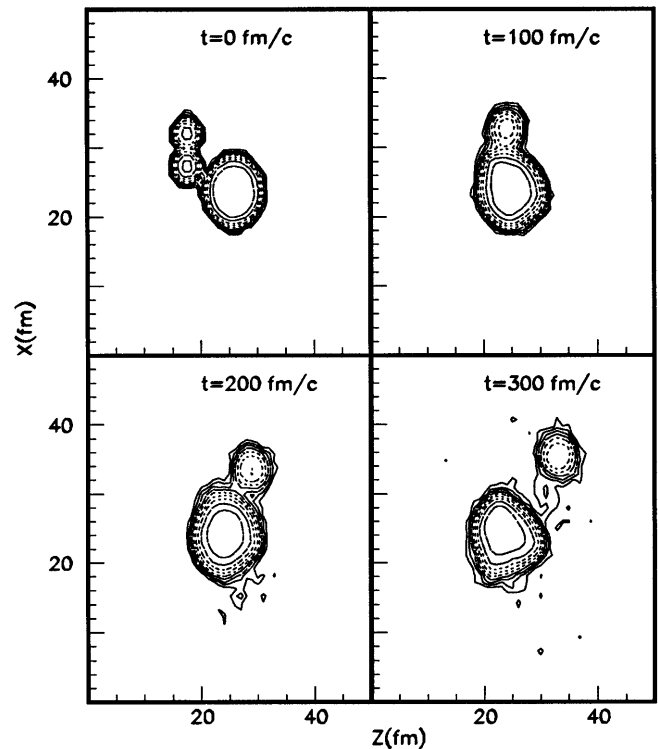


**Fig. 9.** Density plot, at different time, for the system  $^{12}\text{C}^* + ^{64}\text{Ni}$  at  $7.9\text{MeV}/\text{nucleon}$  and  $b=4.7\text{fm}$ , projected on the reaction plane. It has been computed by solving the B.N.V. equation in which the  $^{12}\text{C}^*$  projectile has been described at  $t=0$  like a  $3 - \alpha$  nucleus (see the text)

resentation of the clustered structure. From the picture is also possible to see that the transfer of  $2 - \alpha$  takes place in about  $200\text{fm}/c$ ; at the end we observe the production of an  $\alpha$  particle at about  $6.5\text{MeV}/\text{nucleon}$ .

In Fig. 10a we show the first time derivative of the total dipole along the radial direction, while in Fig. 10b the same quantity for the molecular dipole is also shown. We see that the large amplitude oscillations of the molecular dipole are, in the first  $200\text{fm}/c$ , a large part of the total one ( $70\% - 80\%$ ). Also in this case a connection between the dynamical effect, whose total effect is measured through the total dipole periodicity, and the collective transfer of charge visible through the molecular component, is established.

In particular the mode is excited through the transfer of 2 charge-mass symmetric particles into a charge-mass asymmetric nucleus ( $^{64}\text{Ni}$ ) being the driving force the last term in (6.1).

After about  $200\text{fm}/c$  the molecular component switch-off because the two partners separates while the total one is already relaxed.

We observe also that the particular outgoing channel studied is able to select short time interval in which dynamical effects are the prominent ones because the fusion process is hindered by the dynamics.

Finally in Fig. 10c we display the associated  $\gamma$  emission probability per  $\text{MeV}$ . The peak is centered at  $12\text{MeV}$ ,

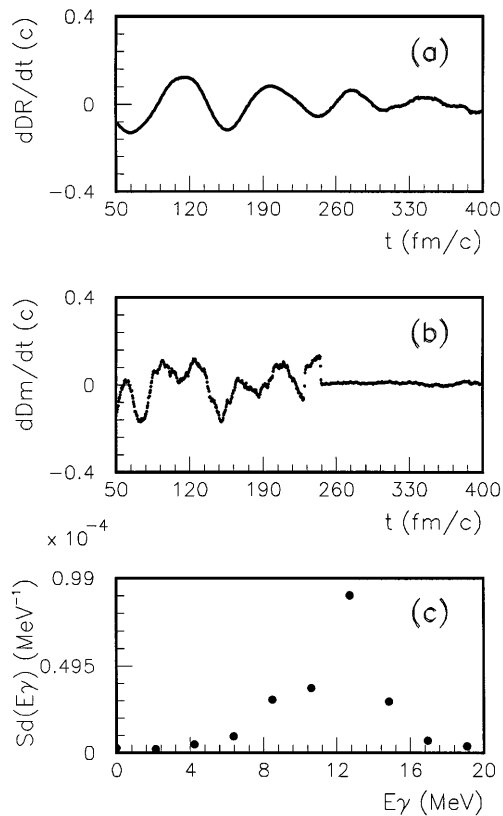


**Fig. 10.** a–c. Results of B.N.V. calculations for the  $^{12}\text{C}^* + ^{64}\text{Ni}$  system at  $7.83\text{ MeV}/\text{nucleon}$  and  $b=4.7\text{ fm}$  in which the  $^{12}\text{C}^*$  projectile has been described at  $t=0$  like a  $3-\alpha$  nucleus (see the text), **a** First time derivative of the total dipole radial component as function of time, **b** First time derivative of the molecular component as function of time, **c** Emission probability distribution as function of the  $\gamma$ -ray energy associated to the total radial component

that is only  $3\text{ MeV}$  higher than the experimental value shown in Fig. 2, but we are able to reproduce the width of about  $3\text{ MeV}$  and a strength value at the peak equal to  $10^{-4}\text{ MeV}^{-1}$ , that is in reasonable agreement with the estimated experimental value.

## 7 Conclusions and outlook

In the present work the nature of the pre-equilibrium  $\gamma$ -emission in nuclear reactions has been discussed. The study performed for the investigated systems has led to a clear distinction between a pre-equilibrium dynamical  $\gamma$ -ray emission due to the equilibration of the proton v.s. neutron motion and a statistical one in which the effect of the slow change in time of the shape degree of freedom has also been included.

A qualitative and semi-quantitative comparison between these two mechanisms of emission has been performed at about  $8\text{ MeV}/\text{nucleon}$ .

Some of the most recent experimental data at this energy [3-5] have been interpreted by studying the dynamics

of the  $^{35}\text{Cl} + ^{64}\text{Ni}$  and  $^{12}\text{C} + ^{64}\text{Ni}$  reactions through the semiclassical kinetic theory.

In particular the “anomalous” character of the high energy  $\gamma$ -ray production evidenced in these reactions has been interpreted as a dipole emission produced by the strongly deformed intermediate system formed during the first 200-300 fm/c of the collision process.

The small experimental values of the widths that characterize the investigated phenomenon and the semiclassical calculations we have done, strongly suggest that at  $8\text{ MeV}/\text{nucleon}$  and for the studied reactions the damping of the collective proton v.s. neutron motion, induced by the charge-mass asymmetry in the entrance channel, displays a “reduced” value as the result of the pronounced time dependence of both the mean field and the nucleon-nucleon collisional rate during the pre-equilibrium stage.

The study performed at different impact parameters has also put in evidence the link between collective transfer of charge and mass in the nuclear reactions and pre-equilibrium emission from the intermediate system. With the analysis done for the interpretation of the experimental data and the above mentioned comparison with the statistical model, we have evidenced the key role played by the reaction mechanisms (fusion, deep-inelastic and massive transfer reactions) on the visibility of this pre-equilibrium effect.

Finally we think that this effect should be the object of further investigations both experimental and theoretical.

In particular we think to be fundamental, to study this phenomenon also in the framework of other theoretical approaches for a global and definitive understanding of its nature. In fact some crucial problems remain opened like, for example, the role played by the classical and quantal fluctuations and the consequences of the non-locality in the mean field. On the other hand we observe that the interpretation of any kind of observed deviation from the statistical model prediction can represent surely a useful test for all the theoretical approaches which aim to the description of the equilibration processes in nuclear dynamics.

## Appendix A

Let us consider a classical system whose total energy at the time  $t = 0$  can be divided in a collective part and a part stored in microscopic degree of freedom. This situation is typical for systems far from the equilibrium, like in the case under study, in which due to the initial large not uniformity in the charge-mass asymmetry, the proton and neutron spheres gain a collective displacement corresponding to  $Dm(0)$  (see equation 3.4). During the time evolution the system evolves from the relatively simple initial configuration to the more complex one in which all the collective energy is shared to a complicated configuration which can be well treated by means of the statistical theory of the equilibrated system.

Let us now divide the collective energy  $E_0^c$  in  $n_S$  intervals  $\Delta\varepsilon_n$ . During the time evolution, due to the dissipation

effects, the collective energy stored in the initial configuration will be dissipated until it will reach the equilibrium value. It is possible then to define  $n_s$  numbers  $P_n$  corresponding to the probability the system will have a collective energy inside the interval  $[E_0^c - (n-1)\Delta\varepsilon_n, E_0^c - n\Delta\varepsilon_n]$  which we represent through a discrete stochastic variable  $\varepsilon_n^c = E_0^c - \frac{n}{2}\Delta\varepsilon_n$ . Moreover it is also possible to define the damping widths (or transition probabilities)  $\Gamma_{n,n'}$  between different intervals.

With this ingredients we can simulate now the dissipation phenomenon by means the evolution of the stochastic discrete variable  $\varepsilon_n^c$  which we assume to follow an homogeneous Markov process. Allowing the system to be open the following set of master equations can be obtained

$$\frac{\partial P_n}{\partial t} = \sum_{k=1}^{n_S} P_k \Gamma_{k,n} - P_n \Gamma_{n,k} - P_n \Gamma_n^\uparrow \quad (\text{A.1})$$

If the intervals are large enough we can assume the following two conditions:

- i)  $\Gamma_{i,j} = 0$  if  $|i - j| > 1$
- ii)  $\Gamma_{i,j} \ll \Gamma_{j,i}$  if  $j < i$

These two conditions have been already used in the well known F.K.K. pre-equilibrium reaction theory [12] and they have been named ‘‘chaining’’ and ‘‘never back’’ hypothesis respectively. In particular due to the way in which we have decomposed the phase space accessible to the system the second condition introduces explicitly the macroscopic irreversibility of the dissipation phenomenon.

In this hypothesis the general solution of the system is:

$$P_n = \sum_{i=1}^{i=n} A_{n,i} e^{-\Gamma_i t} \quad (\text{A.2})$$

with:

$$A_{n,k} = \frac{A_{n-1,k} \Gamma_{n-1,n}}{\Gamma_n - \Gamma_k} \quad k < n \quad (\text{A.3})$$

and

$$\begin{aligned} \Gamma_n &= \Gamma_{n,n-1} + \Gamma_{n,n+1} + \Gamma_n^\uparrow \simeq \Gamma_{n,n+1} + \Gamma_n^\uparrow \\ &= \Gamma_n^\downarrow + \Gamma_n^\uparrow \end{aligned} \quad (\text{A.4})$$

Equation (A.2) represents a recurrence relation for off-diagonal coefficients. The diagonal coefficients can be determined through the initial conditions:

$$P_k(0) = \sum_{i=1}^{i=k} A_{k,i} = \alpha_k \quad k = 1, n_S \quad (\text{A.5})$$

In the actual situation, to describe the physical interaction between two heavy ions, we can assume  $\alpha_k = \delta(k-1)$ .

As an example we consider a partition of the total phase space into three regions. By integrating the solution over the time we get the total probability the system will stay in one of the three classes. This quantity is interesting from an experimental point of view because it is connected with the total yield of  $\gamma$ -ray that the system can produce during all its time evolution. So we get:

$$P_1^T = \frac{1}{\Gamma_1} \quad (\text{A.6})$$

$$P_2^T = \frac{\Gamma_{1,2}}{\Gamma_1 \Gamma_2} \quad (\text{A.7})$$

$$P_3^T = \frac{\Gamma_{1,2} \Gamma_{2,3}}{\Gamma_1 \Gamma_2 \Gamma_3} \quad (\text{A.8})$$

To put in evidence the pre-equilibrium contribution we can make a partial summation obtaining:

$$P_D^T = P_1^T + P_2^T = \frac{1}{\Gamma_D} \quad (\text{A.9})$$

$$P_S^T = P_3^T = \frac{\Gamma_D^\downarrow}{\Gamma_D \Gamma_3} = \frac{\Gamma_D^\downarrow}{\Gamma_D \Gamma_S} \quad (\text{A.10})$$

with:

$$\Gamma_D = \frac{\Gamma_1 \Gamma_2}{(\Gamma_2 + \Gamma_{1,2})} \quad (\text{A.11})$$

$$\Gamma_D^\downarrow = \frac{\Gamma_{1,2} \Gamma_{2,3}}{\Gamma_2 + \Gamma_{1,2}} \quad (\text{A.12})$$

From the above expressions, that obviously can be generalized to more than three steps, we see that the values of  $\Gamma_D$  and  $\Gamma_D^\downarrow$  are effective values i.e. combinations more or less complicated of the parameters characterizing every class even if the  $\Gamma_D$  and  $\Gamma_D^\downarrow$  values so extracted have to be interpreted as average values not able to reproduce the details of the time distribution.

The total probability per unit of energy to emit a  $\gamma$ -ray then can be written as

$$\frac{dP^{T,\gamma}}{dE_\gamma} = \frac{W_S^\gamma}{\Gamma_S} \frac{\Gamma_D^\downarrow}{\Gamma_D} + \frac{W_D^\gamma}{\Gamma_D} \quad (\text{A.13})$$

where  $W_D^\gamma$  and  $W_S$  represent the reduced width for the  $\gamma$ -ray emission for the pre-equilibrium and the equilibrium stages of the process respectively.

## Appendix B

The last stage of the chain, according to the definition given in Appendix A, can give a statistical  $\gamma$ -ray production which is represented by the first term in (4.1). In particular, apart from the ratio  $\frac{\Gamma_D^\downarrow}{\Gamma_D}$ , the factor  $\frac{W_S^\gamma}{\Gamma_S}$  takes into account the statistical decay after the time at which the proton v.s. neutron motion is equilibrated.

At this time the nucleus in general does not have the equilibrium deformation, then some dynamical effects should be considered. Some recent experimental evidences on  $\gamma$ -ray emission [32], seem to confirm this fact. In order to take into account these effects, some authors have used the statistical theory coupled with transport theories (see as an example [33,34]). This coupling is based on the local time equilibrium hypothesis. In the following, by using the same hypothesis, we will use a different approach.

To insert non-stationary effects in the C.N. theory, we have considered explicitly the decay law of the compound nucleus. Then the total probability per unit of energy to

emit a  $\gamma$ -ray from the GDR can be written in the local time equilibrium hypothesis as:

$$S_s(E_\gamma) = \sum_0^{J_{max}} \frac{2J}{J_{max}^2} \int_0^\infty W_S^\gamma(E_\gamma, J, t) e^{-\frac{t}{\tau_{CN}^J}} dt \quad (\text{B.1})$$

(in this case the ratio  $\frac{\Gamma_\beta^J}{\Gamma_D}$  has been set equal to 1). It appears like a weighted mean respect to both the different total angular momenta  $J$  involved in the reaction and the time decay law of the C.N.

The time dependence of the partial width for  $\gamma$  emission is due to the time dependence of the deformation degrees of freedom which give an explicit time dependence for the damping width, for the resonance energies  $E_{GDR}$  along the symmetry axes, for the temperature through deformation energy and moment of inertia.

In (B.1)  $\tau_{CN}$  represents the mean life time of the C.N. (of the order of the mean life for neutron decay). Obviously (B.1) represents the first step contribution to the cascade which is the most prominent one for the GDR  $\gamma$  emission.

For what concerns the description of the deformation we have chosen to describe a nucleus with an axially symmetric prolate shape whose parameters  $\beta = a_2$ ,  $R = R_0(1 + a_2 P_2(\cos(\theta)))$  changes in time through an exponential law (overdamped motion). This choice is well suited to describe processes leading to fusion how can be deduced from dynamical calculation after the equilibration of the proton v.s. neutron motion. This average time dependence is also in agreement with a phenomenological analysis of heavy ion collisions in term of the Fokker-Plank equation (see as an example [35]).

Therefore for each value of the total angular momenta we can write:

$$\beta(t) = \beta_{eq}^J + (\beta_{max}^J - \beta_{eq}^J) e^{-\frac{t}{\tau_\beta^J}} \quad (\text{B.2})$$

where  $\tau_\beta^J$  is the relaxation time for the deformation degree of freedom. By fixing the  $\beta_{max}^J$  value it is possible to take into account the time delay corresponding to the time interval necessary for the equilibration of the proton-neutron collective motion.

By substituting (B.2) in (B.1) and by changing variables we obtain for  $\tau_\beta^J \geq 0$ :

$$\begin{aligned} S_s(E_\gamma) &\cong \sum_0^{J_{max}} \frac{2J}{J_{max}^2} \int_{\beta_{min}^J}^{\beta_{max}^J} \tau_\beta^J W_S^\gamma(E_\gamma, J, \beta) \\ &\quad \times \left( \frac{\beta - \beta_{eq}^J}{\beta_{max}^J - \beta_{eq}^J} \right)^{\frac{\tau_\beta^J}{\tau_{CN}^J}} \frac{1}{\beta - \beta_{eq}^J} d\beta \\ &\quad + \sum_0^{J_{max}} \frac{2J}{J_{max}^2} W_S^\gamma(E_\gamma, J, \beta_{eq}^J) \left( \frac{\beta_{min}^J - \beta_{eq}^J}{\beta_{max}^J - \beta_{eq}^J} \right)^{\frac{\tau_\beta^J}{\tau_{CN}^J}} \end{aligned} \quad (\text{B.3})$$

In expression (B.3) any time dependence has been dropped out. The last term is just the integral contribution in the interval  $[\beta_{eq}^J, \beta_{min}^J]$ . This contribution can be

neglected at the order  $(\beta_{min}^J - \beta_{eq}^J)^{\frac{\tau_\beta^J}{\tau_{CN}^J}}$ , for  $\beta_{min}^J \sim \beta_{eq}^J$ .

Under this condition the quantity:

$$P_\beta^J = \left( \frac{\beta - \beta_{eq}^J}{\beta_{max}^J - \beta_{eq}^J} \right)^{\frac{\tau_\beta^J}{\tau_{CN}^J}} \frac{1}{\beta - \beta_{eq}^J} \quad (\text{B.4})$$

can be interpreted as the probability that the intermediate system with total angular momentum  $J$  will experience a deformation  $\beta$  in the large time interval  $[0, \tau_\beta^J \log(\frac{\beta_{max}^J - \beta_{eq}^J}{\beta_{min}^J - \beta_{eq}^J})]$ .

This procedure can be generalized also by including shape fluctuations. In this case from the statistical theory of non-equilibrated system or from the thermodynamic of finite systems one can get the quantity  $Q(\beta, \langle \beta(t) \rangle)$  i.e. the probability that the system will experience at the time  $t$  the deformation  $\beta$ . Through the folding:

$$\begin{aligned} S_s(E_\gamma) &= \sum_0^{J_{max}} \frac{2J}{J_{max}^2} \int_{\beta'} \int_0^\infty W_S^\gamma(E_\gamma, \beta' J, t) e^{-\frac{t}{\tau_{CN}^J}} \\ &\quad \times Q(\beta', \langle \beta^J(t) \rangle) dt d\beta' \end{aligned} \quad (\text{B.5})$$

(in the case for which  $Q(\beta', \langle \beta^J(t) \rangle) = \delta(\beta' - \langle \beta^J(t) \rangle)$  we get the expressions (B.4) and (B.3)) it is possible to insert the fluctuation effect by integrating over  $\beta'$ . After this by using the time evolution of the mean deformation  $\langle \beta^J(t) \rangle$  in the same way as above, it is possible to express the time integral through an integral over the deformation degree of freedom i.e. it is possible to define a density of strength in the  $\beta$  space and its probability distribution. Obviously these last quantities could be inserted at each step in a MonteCarlo structure producing a fast event generator.

The expression (B.3) has been evaluated for the system  $^{12}\text{C} + ^{64}\text{Ni}$  at  $7.8\text{MeV}/\text{nucleon}$  which corresponds to a temperature of about  $3.03\text{MeV}$ . Dynamical calculation predicts fusion up to an impact parameter  $b \simeq 5.5\text{fm}$ . For the reduced width  $W_S^\gamma(E_\gamma)$  we have used the relation (4.2). The energy dependence of the  $\gamma$  absorption cross section has been described through the following expression [36,37]:

$$\begin{aligned} \sigma_{abs}(E_\gamma) &= \frac{4\pi e^2 \hbar N Z}{m c A} \\ &\quad \times \sum_{j=1}^{j=2} \frac{S_j \Gamma_j E_\gamma^2}{(E_\gamma^2 - E_{GDR}^2(\beta))^2 - (E_\gamma \Gamma_j)^2} \end{aligned} \quad (\text{B.6})$$

The deformation effects have been evaluated for the splitting of the resonance energies in the first order in  $\beta$  following [36]. The deformation changes also the ground state energy of the system and this has been evaluated up to the second order in the  $\beta$  parameter following the liquid drop model. Finite temperature effects have also been included to correct the surface energy coefficient. Moments of inertia have been evaluated according to the rigid rotor formula. The change in the actual temperature  $T(\beta^J)$ , due to these effects, has been taken into account also for the damping width of the GDR  $\Gamma(\beta, T)$  which has been described through a linear dependence from  $T^2(\beta^J)$

**Table 1.** Results of the statistical model parameters obtained through the fit procedure with CASCADE calculations applied to the experimental data shown in Fig. 3 [3]

Kind of fit	a	E1 <sub>GDR</sub>	E2 <sub>GDR</sub>	$\Gamma$ 1 <sub>GDR</sub>	$\Gamma$ 2 <sub>GDR</sub>	S1	S2	CHI <sup>2</sup>
1 Lor.	A/8	17.0±0.5	–	9.6±1.0	–	1.4±0.2	–	2.39
2 Lor.	A/8	17.8±0.5	13.2±0.5	7.0±1.0	4.1±1.0	0.62±0.2	0.38±0.2	11

according to [38]. The parameters of the linear relation have been chosen by imposing the following conditions;  $\Gamma(0,0) = 5.5MeV$  and  $\Gamma(0,3.03) = 11MeV$ . The last condition is in agreement with the parameters obtained from CASCADE calculations (see Fig. 3 and Tab. 1)

In Fig. 5 we show the obtained results. From the preliminary dynamical study of the system, we have verified that after the proton v.s. neutron motion equilibration time (about 200 fm/c), i.e. when the statistical contribution becomes effective, the dependence on the total angular momentum of the parameters describing the deformation relaxation phenomenon can be neglected.

We have estimated a mean life time for the C.N. system of about 850 fm/c. In this figure we compare the results obtained for  $\beta_{max} = 0.5$   $\beta_{max} = 0$  ( $\beta_{eq} = 0$ ) for different deformation relaxation times  $\tau_\beta$ . In the picture are shown also the extreme cases relative to stationary processes (i.e.  $\tau_\beta = +\infty fm/c$ ). As expected the yield for  $\beta_{max} = 0.5$  is peaked at an energy lower than the value corresponding to the spherical case. The total contribution is about one half respect to the case of  $\beta_{max} = 0$ . This is an effect due to the symmetry of the deformation and to the temperature. In fact even if to the mode at lower energy corresponds only one third of the total strength in an equilibrated system, this mode has the bigger weight in the total probability respect to the transversal one (its resonance energy has been evaluated from the lower resonance energy, by supposing the weighted mean equal to the resonance energy of the spherical system), because of the temperature dependent exponential factor.

The other cases for which  $\beta_{max} = 0.5$  but for which the deformation relaxation time has finite values, show an intermediate behaviour which depends on the ratio  $R = \frac{\tau_\beta}{\tau_{CN}}$ . The case relative to the greatest R value reported ( $R=1$ ) is obviously the more similar to the stationary case.

In general the peak position is not very much sensitive to the deformation. This is due mainly to the large values of  $\Gamma_j$  and to the exponential fall off in the spectra rising from the level density factor. Moreover the distribution law in the deformation variable, for  $\frac{\tau_\beta}{\tau_{CN}} < 1$ , will give the largest weight to the equilibrium deformation. This last condition reduces the sensitivity of the peak intensity respect to the ratio R for  $R < 0.4$

A last observation on the shape of the spectra displayed is that in all cases the F.W.H.M. is about 10 – 11MeV. This enables us to think that “Pre-equilibrium-Statistical” GDR emission, after the equilibration of the neutron v.s. proton motion, in processes leading to fusion, can not explain the narrow peaks observed in the data shown in the Figs. 1 and 2.

To complete our estimations on this kind of emission we want to discuss briefly the case of very large deformation. As above we concentrate our attention on one of the system for which an enhancement of high energy  $\gamma$ -rays has been detected.

For  $^{35}Cl + ^{64}Ni$  at  $7.8MeV/nucleon$  an extra yield of  $\gamma$ -rays has been detected in coincidence with deep inelastic reactions. As well established from a lot of experimental evidences this kind of process evolves through the formation of a very deformed system in dump-bell shape; the so called dinuclear system will rotate at high angular momentum until it will break-up. Moreover, during this time, we can suppose that the deformation remains practically unchanged ( $\tau_\beta \rightarrow +\infty$ ).

Starting from this considerations we have tried to evaluate the high energy  $\gamma$  rays production from such a system by using the formula (B.3).

To this aim we have evaluated the deformation energy  $E_{def}$  as:

$$E_{def} = E_{fs} - Q_{fus} \quad (B.7)$$

where  $E_{fs}$  is the energy due to the asymmetric fission evaluated following [36].  $Q_{fus}$  is the Q-value for the fusion process.

To evaluate the rotational energy we have considered the moment of inertia of a rigid rotor in a sticking configuration. As in the previous estimations all the collective energy is subtracted from the total excitation energy giving rise to a lower effective temperature.

In Fig. 6 we report the result of this estimations. In this case the free parameter is the value of the resonant energy correspondent to the radial mode  $E_{GDR}$ . The calculations are relative to one value of the total angular momentum ( $J = 76\hbar$ ). To this contribution we have attributed an unitary weight. In this way the obtained emission probability, taken as representative of the statistical emission rate in D.I.C.(see the text), can be compared with exclusive measurements.

As it is possible to observe, there is a strong reduction of the strength as compared with the more central collisions shown in Fig. 5. This reduction is of about two order of magnitude and it is due to the lower effective temperature obtained by subtracting the large deformation energy and rotational energy to the total one. To obtain a peak centered around 10MeV (as suggested from the experiments) it is necessary to set a value of  $E_{GDR}$  inside the interval 12–14MeV. The F.W.H.M. of the distribution increases by increasing the resonance energy because in this case higher temperature are favoured. For  $E_{GDR}$  equal 12 and 14MeV we obtain a F.W.H.M. of 8 and 10MeV respectively.

Also in this case we can conclude that this kind of emission can not be the source of the over production we are discussing.

One of us (M.P) is grateful to Dr. A.Bonasera and Dr. F.Gulminelli which have initiated him in to the Semiclassical Kinetic Theories. We wish also to thank Prof. M.Di Toro for useful discussions.

## References

1. N. Alamanos and F. Auger, *Ann. Phys. Fr* 16, 41 (1991)
2. C. Agodi et al., *Phys. Lett. B* 308, 220 (1993).
3. F. Amorini, M. Cabibbo, G. Cardella, A. DiPietro, P. Figuera, A. Musumarra, M. Papa, G. Pappalardo, F. Rizzo, S. Tudisco, Submitted to *Phys. Rev. C*
4. F. Rizzo, F. Amorini, M. Cabibbo, G. Cardella, A. DiPietro, P. Figuera, A. Musumarra, M. Papa, G. Pappalardo, S. Tudisco, *Proceedings of the International Symposium on Large-Scale Collective Motion of Atomic Nuclei*, Brolo, Italy, October 15-19, 1996 pg. 487; Ed. by G. Giardina, F. Fazio, M. Lattuada
5. L. Campaiola et al, *Nucl. Phys. A*583, 119 (1995)-*Z. Phys. A*352, 421 (1995)
6. V. V. Kamanin, A. Kugler, Yu. G. Sobolev and A. S. Fomichev, *Z. Phys. A*337, 111 (1990)
7. A. Musumarra, G. Cardella, A. Di Pietro, S. L. Li, M. Papa, G. Pappalardo, F. Rizzo, S. Tudisco, J. P. S Van Schagen, *Nucl. Instrum. Methods A*370, 558 (1996)
8. S. Flibotte et al, *Phys. Rev. Lett* 77 1448 (1996)
9. C. Yanhuang, M. Di Toro, M. Papa, A. Smerzi, Z. Jiquan, *Proceeding of the Int. Conf. on Dynamical Features of Nuclei and Finite System*, Barcelone 1993, ed by X. Vinas
10. Ph. Chomaz, M. Di Toro and A. Smerzi, *Nucl. Phys. A*563, 509 (1993)
11. V. Baran, M. Colonna, M. Di Toro, A. Smerzi, *Nucl. Phys. A*600,111, (1996)
12. K. W. Mc. Voy and X. T. Tang, *Phys. Rep.* 94, 139 (1983) and reference therein
13. D. M. Brink, *Nucl. Phys. A*519, 3c (1990)
14. P. F. Bortignon, A. Bracco, D. M. Brink and R. A. Broglia, *Phys. Rev. Lett* 67 3360 (1991)
15. F. Puhlhofer *Nucl. Phys. A*280, 267 (1977)
16. R. A. Broglia and W. E. Ormand, *Nucl. Phys. A*482 141c (1988)
17. W. Noremborg, *Phys. Lett.* 104B 107 (1981)
18. J. W. Negle, *Rev. Mod. Phys* 54 113 (1982)
19. W. Cassing and W. Norenberg, *Nucl. Phys. A*408 467 (1983)
20. W. Cassing, *Nucl. Phys. A*438 253 (1985)
21. A. Bonasera, F. Gulminelli, S. Molitoris, *Phys. Rep.* 243, 1 (1994) and reference therein
22. M. Di Toro, G. Gregoire, *Z. Phys. A*320 321 (1983)
23. G. Gregoire et al, *Phys. Rev. C* 2594 (1998)
24. M. Zielinska-Pfabé, C. Gregoire, *Phys. Rev. C* 37 2594 (1988)
25. I. N. Mikhailov, T. I. Mikhailova, M. Di Toro, V. Baran, *Nucl. Phys. A*372 (1996) 151
26. A. Bonasera and A. Iwamoto *Phys. Rev. Lett.* 78 187 (1997)
27. E. Gadioli, *Phys. Lett B* 394 20Feb (1977) , *Proceedings of the 8th international conference on nuclear reaction mechanisms*, Varenna, Italy, June 7-14, 1997 pg. 368 Ed. by E. Gadioli
28. M. Takamoto, *Proceedings of the 8th international conference on nuclear reaction mechanisms*, Varenna, Italy, June 7-14, 1997 pg. 616, Ed. by E. Gadioli
29. Hisashy Horiuky et al, *Supp. Prog. Theor. Phys.* 52, 89 (1972) , *Supp. Prog. Theor. Phys.* 52, 228 (1972)
30. Y. Abe, J. Hiura and H. Tanaka, *Prog. Theor. Phys.* 49, 800 (1973)
31. D. M. Brink, *International School of Physics "Enrico Fermi"*, XXXVI 247 (1966)
32. M. Thoenesen J. R. Beene, F. E. Bertrand, C. Baktash, M. L. Halbert, D. J. Horen, D. G. Saranties, W. Spang, and D. W. Stracener, *Phys. Rev. Lett.* 70, 4055 (1993)
33. P. Grange, H. C. Pauli and H. A. Weidenmuller, *Z. Phys A*296, 107 (1980)
34. K. Pomorski, J. Bartel, J. Richert, and K. Dietrich, *Nucl. Phys. A*605, 267 (1996) , and reference therein
35. G. Wolshin, W. Noremborg, *Z. Phys. A*290, 209 (1979)
36. W. D. Myers and W. J. Swiatecki, *Nucl. Phys.* 81, 1 (1966)
37. K. A. Snover, *Ann. Rev. Nucl. Part. Sci* 36, 545 (1986) and reference therein
38. A. Smerzi, A. Bonasera and M. Di Toro, *Phys. Rev. C* 44, 1713 (1991)